

Analyzing powers and isotope ratios for the $^{nat}\text{Ag}(\bar{p}, \text{intermediate-mass fragment})$ reaction at 200 MeV

E. Renshaw, S. J. Yennello, K. Kwiatkowski, R. Płaneta,* L. W. Woo,[†] and V. E. Viola

Department of Chemistry and Indiana University Cyclotron Facility, Indiana University, Bloomington, Indiana 47405

(Received 6 June 1991)

Analyzing powers and isotope ratios have been measured for ejectiles with $Z \leq 7$ emitted at forward angles in the 200-MeV $\bar{p} + ^{nat}\text{Ag}$ reaction. The observed analyzing powers are consistent with zero, and thus do not provide evidence for a significant contribution from cluster knockout, or similar direct formation mechanisms. Fragment kinetic-energy spectra above the Coulomb peak are compared with a coalescence calculation. The isotopic composition of the elemental kinetic-energy spectra is found to favor $N/Z \geq 1$ nuclei for fragment energies near the exit-channel Coulomb energy, whereas species with $N/Z \leq 1$ are more abundant in the high-energy spectral tails. This behavior is consistent with the prediction of an accreting source calculation.

I. INTRODUCTION

The emission of intermediate-mass fragments (IMF, $3 \leq Z \leq 15$) from reactions induced by intermediate-energy protons below about 1 GeV has been shown to proceed via both statistical decay and fast, nonequilibrium mechanisms [1–3]. The equilibrated component of the spectra is most apparent at backward emission angles and can be well described by standard statistical decay models [4–7], at least in a qualitative sense. In contrast, nonequilibrium emission, which dominates the forward-angle spectra, remains poorly understood [1–3]. These ejectiles are characterized by rapidly rising cross sections near zero degrees, suggesting formation on a very short time scale. Further, spectra for ejectiles as heavy as neon extend to momenta over two times the beam momentum. By way of reference, this momentum corresponds approximately to a direct cluster knockout in which the incident proton is scattered at 180° , or, alternatively, to a Coulomb repulsion energy for binary decay of two touching spheres in which the nuclear radius is given by $R \approx 0.6A^{1/3}$ fm. While neither of these mechanisms seems realistic, especially for heavy fragments such as oxygen and neon, the comparison illustrates the difficulty in attempting to account for these fast collective processes.

The question of time scales is an important one for understanding the mechanisms responsible for the emission of nonequilibrium complex fragments from highly excited nuclear matter. In principle, the use of transversely polarized beams and measurement of a finite analyzing power associated with any portion of the fragment spectra would provide support for a direct mechanism. Calculations [8,9] have shown that direct cluster knockout at intermediate energies should be accompanied by meaningful analyzing powers for ^4He ejectiles from medium-mass target nuclei. Measurements of the reactions $^{93}\text{Nb}(\bar{p}, ^4\text{He})$ at 65 MeV [10] and $^{90}\text{Zr}(\bar{p}, ^4\text{He})$ at 72 MeV [11] have previously provided evidence for finite analyzing powers for the most energetic component of the ^4He

spectrum. At small angles, negative analyzing powers of the order $A(\theta) \approx -0.05$ – -0.1 were observed; with increasing angle the analyzing powers increased systematically, becoming zero near 30° and reaching values of $A(\theta) \approx 0.2$ at angles beyond 60° . In contrast, for low-energy ^4He ejectiles near the Coulomb barrier energy, the analyzing-power results were consistent with zero at all angles. A satisfactory fit to these data has been obtained with the multistep direct reaction model of Tamura *et al.* [12].

Green *et al.* [9] investigated $^3,^4\text{He}$ emission at angles of 60° and greater in bombardments of a ^{nat}Ag target with transversely polarized protons with energies of 237, 445, and 518 MeV. No statistically significant analyzing powers were observed, leading the authors to conclude that the observed yields at higher energies could not be accounted for by a direct knockout mechanism. However, since the measurements of Green *et al.* were performed at angles of 60° or greater, the observed spectra may be dominated by equilibrated emission, for which a zero analyzing power would be expected.

In the present experiment we have sought to investigate the possible importance of direct one-step mechanisms to the complex fragment yields at very forward angles, using a transversely polarized beam of 200-MeV protons. The experiment was designed to measure analyzing powers for isotopically separated ejectiles from H to N, and charge-identified fragments up to Mg. The fragment spectra are compared with a coalescence model based on experimental proton spectra. These data also permit comparison of the spectra and yields for individual isotopes which make up the total charge distribution for a given element. Previous studies have shown that the spectral shapes for a given element vary with the N/Z ratio of the ejectile [13]. This has led to the suggestion that isotope ratios may provide useful insights into the formation mechanism [14]. The isotope ratios observed in these studies are examined in the context of an accreting-source calculation [15].

II. EXPERIMENTAL PROCEDURES

The experiment was conducted at the Indiana University Cyclotron Facility with a 200-MeV polarized proton beam of average intensity 15–30 nA and spot size ≤ 2 mm in diameter. The average transverse polarization (typically 74%) was reversed at 25-s intervals and monitored by a beam-line polarimeter. High-purity silver targets of thicknesses 1.22 and 1.62 mg/cm² were bombarded in a 162-cm-diam scattering chamber, and were alternated during the experiment to minimize any effects of carbon buildup. Runs with a blank-target frame and a carbon target were performed to evaluate possible contamination of the spectra from beam halo and/or light-element impurities in the target. From the spectra in Fig. 1 it is clear that such contaminants are small.

Measurements for He ejectiles and intermediate-mass fragments (IMF, $3 \leq Z \leq 12$) were performed with a pair of particle-identification/time-of-flight telescopes, each consisting of an axial-field gas-ionization chamber operated at 20 Torr of CF₄ gas, followed by two silicon surface-barrier detectors of thicknesses 90 μ m and 1 mm, respectively, and a 5-mm lithium-drifted-silicon detector. Time of flight was measured with respect to the beam RF, which provided a timing resolution of ~ 300 ps. The two telescopes were placed symmetrically at $\pm 9^\circ$ with respect to the beam axis in one experiment and $\pm 15^\circ$ in another. Each detector telescope subtended a solid angle of 4.11 msr, as defined by a brass collimator of internal diameter

17.9 mm. Light charged particles (H and He) were studied separately with a telescope consisting of a 1-mm silicon detector followed by a 127-mm NaI crystal. A brass collimator of internal diameter 174 mm defined a solid angle of 1.77 msr.

All signals were processed via standard NIM and CAMAC electronics modules. Because $\geq 90\%$ of the events were H and He ions, a light-ion rejection circuit was set up in hardware to veto these events for the IMF studies. Light-ion data were taken in separate runs with this circuit removed. Data were acquired on a VAX 11/750 computer using the XSYS data-acquisition program [16]. Electronic and computer deadtimes were monitored with a randomly triggered pulser system and were accounted for in the data analysis. Replay was also performed with the XSYS program.

III. RESULTS AND DISCUSSION

Energy spectra for $Z = 3-6$ fragments detected at 15° are shown in Fig. 1. Spectra at 9° are similar in shape, with somewhat higher cross sections. Since the data in both telescopes were found to be identical within statistics, they are combined here for cross-section purposes. The spectra are Maxwellian in shape for the lower- Z fragments, evolving to nearly Gaussian-shaped distributions for higher Z values. Examination of the high-energy tails of the IMF spectra leads to an observation seen only in light-ion-induced reactions at forward an-

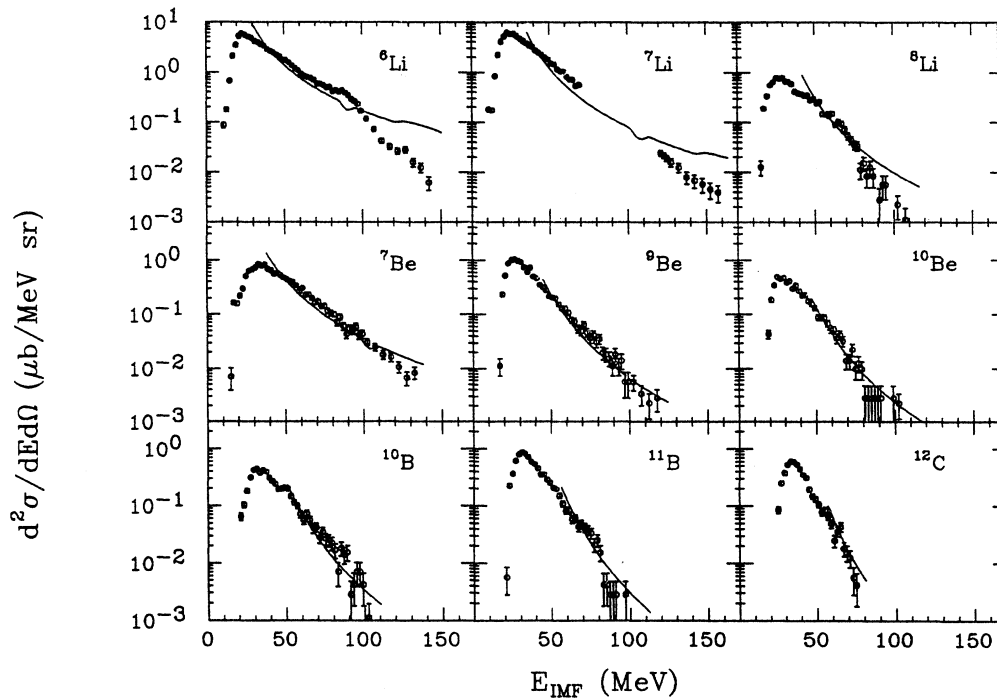


FIG. 1. Kinetic-energy spectra of IMF's, as indicated on figure, for the 200-MeV $\bar{p} + {}^{\text{nat}}\text{Ag}$ reaction at an emission angle of 15° . Solid line is the result of a coalescence fit to experimental proton spectra, using parameters listed in Table I.

gles; i.e., the spectra extend up to momenta corresponding to over two times that of the beam. Based on Coulomb repulsion arguments for binary decay, this corresponds to a charge separation of about 5 fm ($r_0=0.6$ fm) for the fragment and residual nucleus, as compared to a value of 10 fm for two touching spheres based on fission systematics. Thus, simple Coulomb repulsion seems an unlikely mechanism to explain these high-energy events. Alternatively, one could account for these energetic complex fragments in terms of a very fast one-step mechanism; e.g., a direct pickup reaction, or cluster knockout with the projectile scattered near 180° .

A possible signature for the existence of direct one-step processes would be the observation of finite analyzing powers for reactions induced by polarized beams. Here, the analyzing power $A_y(\theta, E)$ is given by

$$A_y(\theta, E) = (1/P)[N(\uparrow) - N(\downarrow)]/[N(\uparrow) + N(\downarrow)], \quad (1)$$

where $N(\uparrow)$ [$N(\downarrow)$] is the number of fragments emitted during reactions induced by protons with spins aligned parallel [antiparallel] to the polarization axis, and P is the average transverse polarization of the beam. Previous calculations [8,9] have indicated that significant analyzing powers might be present for the direct knockout of $^3,4\text{He}$ ejectiles in the $\bar{p} + \text{natAg}$ reaction at intermediate energies. Green *et al.* [9] failed to observe such an effect at angles greater than 60° in studies with 237–518-MeV

polarized protons. The present study was designed to investigate the analyzing-power dependence at very forward angles and to extend the database to IMF spectra as well.

Analyzing powers as a function of observed fragment energy are shown in Fig. 2 (at 9°) and Fig. 3 (at 15°) for several ejectiles. At 9° , all ejectiles with the exception of protons yield analyzing powers consistent with zero, within statistics. For protons, the measured analyzing powers are similar to those reported in previous (\bar{p}, p') studies at forward angles [10,17]: i.e., for low-energy protons the analyzing powers are approximately zero; in the continuum region values of $A(\theta) \approx 0.1-0.2$ are observed, and for the highest energies large $A(\theta)$ values are found, presumably associated with specific spectroscopic states that are unresolved in this experiment. The data at 15° in Fig. 3 are consistent with zero analyzing power for all fragment energies. The same is true near the Coulomb peaks and for the high-energy tails of the spectra observed at 9° . For Li-C fragments in the energy region from 40 to 70 MeV, there appears to be possible evidence for a small positive analyzing power, $A(\theta) \approx 0.1$. However, since these very forward spectra contained some pileup events, it is hard to make a convincing case that this observation is evidence for a positive analyzing power. Thus, unless both angles selected for these studies correspond to points where $A(\theta) = 0$, the measured values of the fragment spectra and analyzing powers do

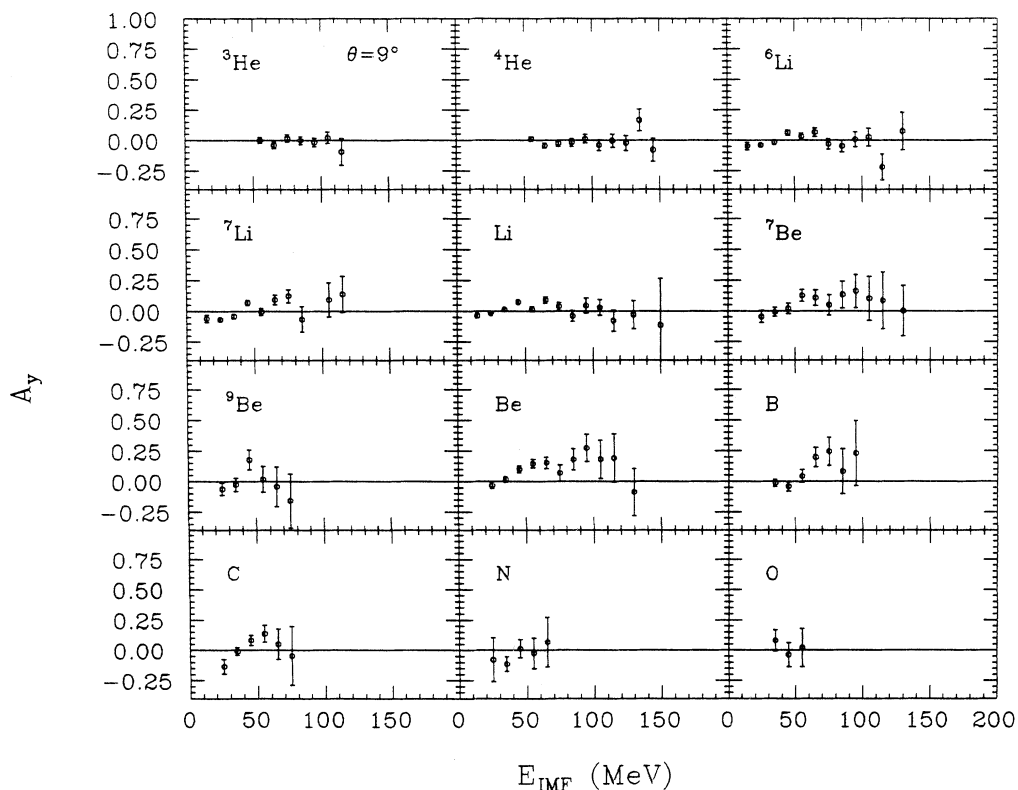


FIG. 2. Analyzing powers for helium and IMF's emitted at 9° for the 200-MeV $\bar{p} + \text{natAg}$ reaction as a function of fragment energy.

not provide convincing evidence for a one-step direct pickup or cluster knockout reaction mechanism as a significant contributor to the complex fragment yields, even at very forward angles. This result is consistent with the earlier conclusions of Ref. [9].

In an effort to examine possible alternative mechanisms for the formation of highly energetic complex fragments, the coalescence model [18,19] has been applied to the energy spectra at 15° . Experimental proton spectra have been used as input to this model for both the proton and neutron distributions; the fits are shown in Fig. 1 as solid lines. Below proton energies of 5–6 MeV the proton spectra are not well defined, thus limiting the fit below a value of $E/A = 5$ MeV. The coalescence momentum P_0 which parametrizes this model was determined with a chi-squared minimization routine to provide a best fit to the data. From the value of P_0 , the interaction zone radius was calculated as in Ref. [19]; these results are presented in Table I. The coalescence momentum (~ 240 – 280 MeV/ c) is found to increase systematically with ejectile mass, while the reverse trend is observed for the interaction zone radius (~ 1.95 – 1.70 fm). The calculation fits the tails of the IMF spectra rather well, yielding interaction zone radii of about 2 fm, much smaller than the radius of the composite systems. In the framework of this model, the results for the source radii are consistent with a mechanism in which the incident pro-

TABLE I. Coalescence and interaction zone radii.

| Fragment | P_0 (MeV/ c) | R (fm) |
|------------------|-------------------|----------|
| ^6Li | 242 | 1.95 |
| ^7Li | 256 | 1.80 |
| ^8Li | 247 | 1.85 |
| ^7Be | 243 | 1.91 |
| ^9Be | 260 | 1.80 |
| ^{10}Be | 265 | 1.84 |
| ^{10}B | 267 | 1.70 |
| ^{11}B | 279 | 1.67 |
| ^{12}C | 280 | 1.72 |

ton interacts with only a localized region of the target nuclear matter density before emission of complex fragments occurs.

Values for the energy-integrated cross sections are shown in Fig. 4 and tabulated in Table II for $Z = 3$ – 12 fragments detected at 15° . These results are in general agreement with those obtained by Green *et al.* [2] at 210 MeV at an emission angle of 20° . The data can be fit using a power law:

$$d\sigma(Z)/d\Omega \propto Z^{-\tau}, \quad (2)$$

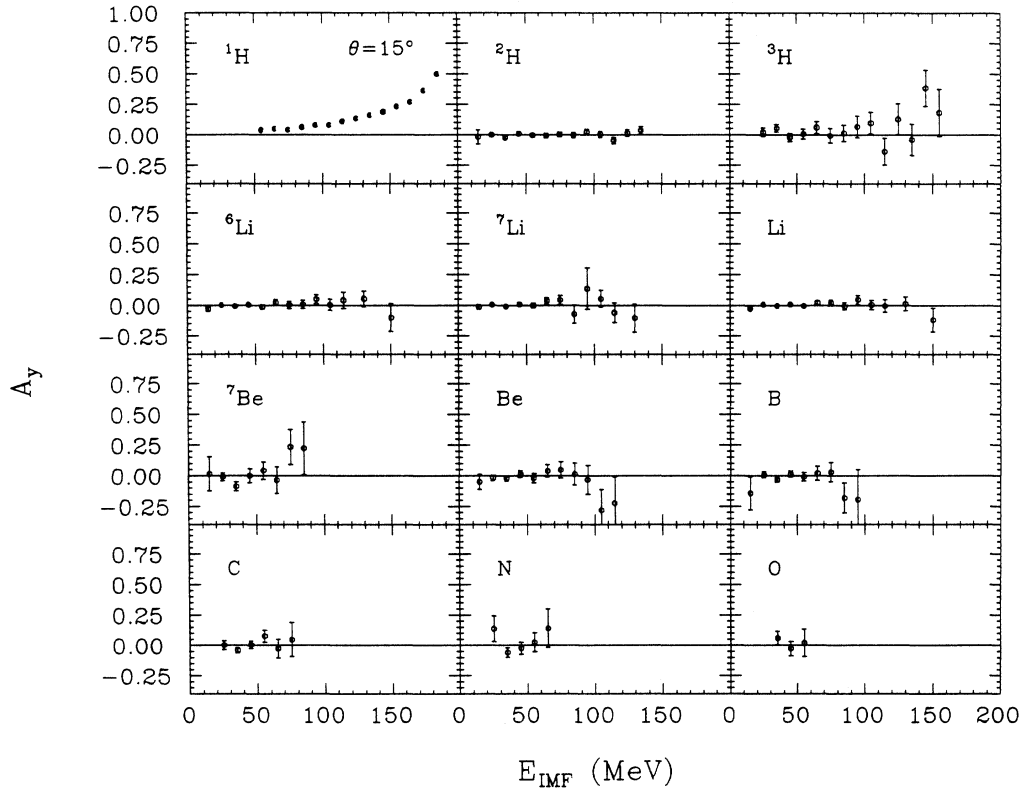


FIG. 3. Analyzing powers for hydrogen nuclei and IMF's emitted at 15° for the 200-MeV $\bar{p} + \text{natAg}$ reaction as a function of fragment energy.

TABLE II. IMF energy-integrated cross sections.

| Fragment | $d\sigma/d\Omega$ ($\mu\text{b}/\text{sr}$) |
|----------|---|
| Li | 360 ± 25 |
| Be | 70 ± 5 |
| B | 35 ± 3 |
| C | 22 ± 2 |
| N | 5.9 ± 0.4 |
| O | 3.2 ± 0.3 |
| F | 1.4 ± 0.2 |
| Ne | 1.3 ± 0.2 |
| Na | 0.74 ± 0.08 |
| Mg | 0.66 ± 0.07 |

yielding a value of $\tau=4.7$ for a fit from $Z=3$ to 10. This forward-angle value is somewhat larger than the values of $\tau=4.0$ for the angle-integrated charge distribution because nonequilibrium emission dominates the cross section at 15° . Equilibrium emission exhibits distinctly smaller τ values [3], thus lowering the average value for the sum of the two components.

The isotopic composition of elemental IMF yields may also possess important information concerning the reaction mechanism [14]. An equilibrated system should preferentially emit fragments which reflect both the N/Z ratio of the composite system and the most energetically favored pathway for decay. This should be independent of fragment kinetic energy. For the $p + \text{Ag}$ system the N/Z ratio is $N/Z \approx 1.27$; thus, the primary fragment yields should favor neutron-excess isotopes. On the other hand, nonequilibrium IMF formation may be more strongly influenced by the projectile nucleon(s), leading to species with N/Z ratios closer to unity. Without some knowledge of the excitation energies of the primary fragments, it is difficult to assess the influence of particle decay on the observed spectra. Nevertheless, to first order, one would expect a general trend that would favor neutron-excess species for equilibrated emission and

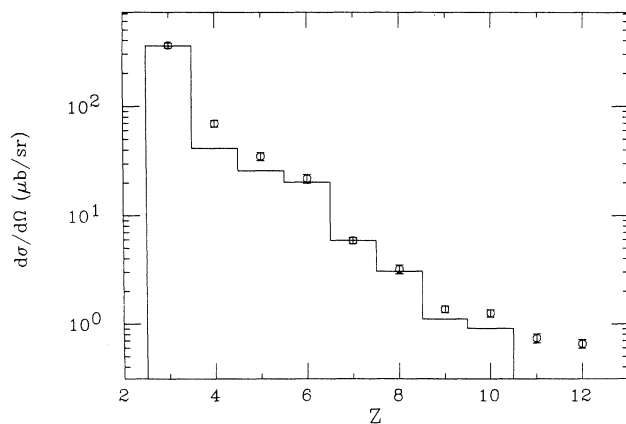


FIG. 4. Elemental differential cross sections for IMF's emitted at 15° in the 200-MeV $\bar{p} + \text{natAg}$ reaction; measured points (O) and accreting source calculation [13] (histogram), as described in text.

$N/Z \lesssim 1$ for nonequilibrated ejectiles.

Isotope ratios, defined here as the yield of a given isotope to the total elemental yield, are presented as a function of IMF kinetic energy for $Z=3-7$ fragments in Fig. 5, and are consistent with the above predictions. For fragment energies near the Coulomb peak, beta-stable and neutron-excess isotopes are the most abundant species, consistent with a picture in which at least partial equilibration has been achieved prior to IMF emission. In general, the yield pattern follows Q -value systematics; the one major exception is for the beryllium isotopes, where ^7Be is anomalously high. As the fragment energy increases, the probability for emitting isotopes with $N/Z \leq 1$ grows in importance, especially for $Z=3-5$ fragments. Thus, the most neutron-deficient isotopes of a given element appear to be identified with the nonequilibrium component of the fragment yields. Similar behavior has been seen in heavy-ion-induced reactions [14,20,21] and has been interpreted in terms of different emission mechanisms being dominant in different parts of the spectra.

In Fig. 5 the observed isotopic ratios are compared with the predictions of an accreting-source model [15,22]. The parameters of the model—accretion rate, Fermi energy, and source size—were fixed by requiring a fit to the elemental differential cross-section distribution at the angle of observation. This comparison is shown in Fig. 4 for an accretion rate of 2.0 nucleons/(fm/c), a Fermi energy of 22 MeV and an initial source size of eight nucleons. The results of the calculation are relatively insensitive to accretion rate and source size; for example, an accretion rate of 4.0 nucleon/(fm/c) and source size of

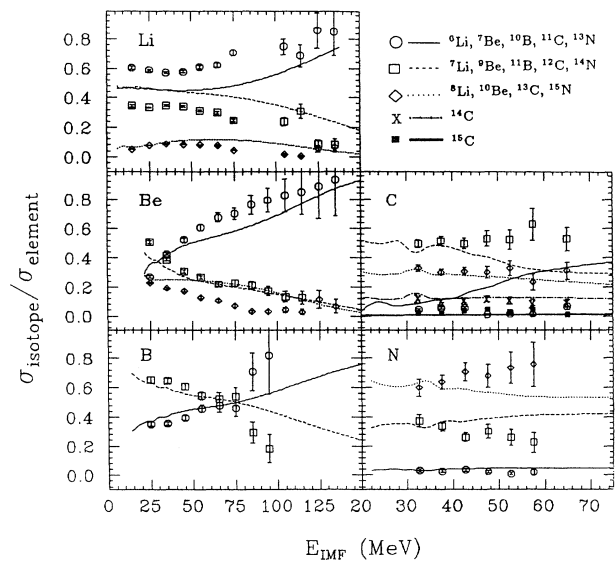


FIG. 5. Ratio of individual isotopic yields to total element yield for Li, Be, B, C, and N fragments observed at 15° as a function of IMF energy. Lines are the result of an accreting-source calculations [13], as identified in the figure. Nuclides are identified by key at upper right.

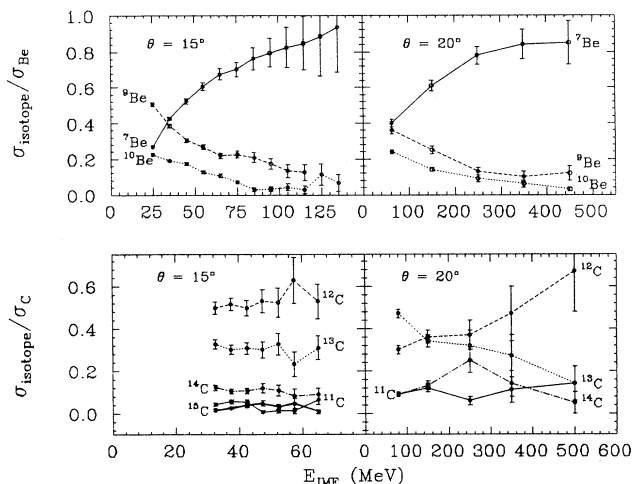


FIG. 6. Comparison of isotopic yield ratios for Be and C fragments at 15° from the 200-MeV $\bar{p} + \text{natAg}$ reaction with corresponding ratios for the $E/A=60$ MeV $^{14}\text{N} + ^{14}\text{Ag}$ reaction [18] measured at 20° . Lines are to guide the eye. Legend: ^7Be , ^{11}C (—); ^9Be , ^{12}C (---); ^9Be , ^{12}C (⋯); ^{14}C (— · — · —) and ^{15}C (—).

four nucleons yields similar predictions. The Fermi energy is more sensitive; an increased Fermi energy produces a flatter charge distribution (lower τ values). In the comparison shown in Fig. 5, no attempt has been made to account for sequential decay of excited fragments heavier than ^5Li ; i.e., we compare theory directly with experimental data.

As observed in Fig. 5, the model qualitatively reproduces the trends observed in the data for $Z=3-5$ fragments. For heavier fragments the preference for the growth of neutron-deficient ejectiles in the high-energy tails of the spectra is much less pronounced. This may in part be due to the fact that with increasing atomic number, the ratio of equilibrated to nonequilibrated IMFs increases [3], thus favoring $N \geq Z$ fragments.

These isotope effects are similar to those for the reaction $E/A=60$ MeV $^{14}\text{N} + \text{natAg}$ [20,21]; a typical comparison for Be and C fragments is shown in Fig. 6. Both reaction systems display similar behavior, suggesting a possible common formation mechanism for nonequilibrium IMF's in both heavy- and light-ion-induced reactions. These data also demonstrate that analysis of elemental spectra in terms of slope temperatures involves significant averaging. For example, a Maxwellian fit to the Be spectra in Fig. 1 yields values of $T=13 \pm 0.5$ MeV for ^7Be and $T=9.5 \pm 0.5$ MeV for ^{10}Be . Similar effects are present in isotopically resolved IMF spectra obtained with ^{14}N projectiles as well [21].

IV. CONCLUSIONS

Previous studies of the $p + \text{natAg}$ reaction between 161 and 480 MeV have shown that both equilibrium and nonequilibrium mechanisms are needed to explain IMF emission [1-3]. The equilibrium component can be explained in terms of statistical decay, but the physics of the nonequilibrium component is not well understood. The major goal of this study was to explore IMF formation at very forward angles (9° and 15°) where nonequilibrium emission is dominant.

To search for evidence of a direct one-step reaction mechanism, the effect of beam polarization on the 200-MeV $\bar{p} + \text{natAg}$ reaction was examined. Analyzing powers were measured, but did not yield convincing evidence to support an IMF formation mechanism involving quasifree knockout or similar direct processes. Thus, we conclude that nonequilibrium complex fragment emission proceeds via a reaction mechanism in which the projectile undergoes multiple collisions with the nucleons in the target nucleus, and a direct one-step reaction mechanism does not contribute significantly to the IMF yields.

The energy spectra were fit with a coalescence model which provides a good description of the high-energy tails of the IMF spectra. An interaction zone radius was extracted and found to be slightly less than 2 fm for the fragments modeled. This implies a source size smaller than the compound nucleus, and thus supports a localized nonequilibrium emission mechanism.

Isotope ratios for lighter Z fragments ($Z=3-5$) suggest that different components of the energy spectra may arise from different mechanisms. For fragment energies near the Coulomb barrier, equilibrated emission is indicated by a preference for isotope ratios with $N/Z \geq 1$, as expected on the basis of decay energetics and the N/Z composition of the composite system. At higher energies, a nonequilibrated mechanism is reflected by isotope ratios weighted more heavily toward neutron-deficient products. For higher Z fragments, the isotope ratios are essentially independent of energy, an effect that is most likely due to the greater importance of the longer interaction times required to emit these fragments.

In summary, these results support a nonequilibrium reaction mechanism for the emission of energetic IMFs at very forward angles. The analyzing-power data, however, do not provide evidence for a direct cluster knockout, or similar, one-step reaction mechanism.

We acknowledge the excellent support of the IUCF operations and experimental support crews. The high-purity silver targets were fabricated by Bill Lozowski, and N.R. Yoder provided valuable support with the data acquisition and analysis program. This research was supported by NSF Grant No. PHY-87-14406 and the U.S. Department of Energy Grant No. DE-FG02.88ER.40404.A000.

*Present address: Institute of Physics, Jagiellonian University, Reymonta 4, Krakow, Poland.

†Present address: Sabbagh Associates, Bloomington, IN 47401.

- [1] R. E. L. Green and R. G. Korteling, *Phys. Rev. C* **22**, 1594 (1980).
- [2] R. E. L. Green, R. G. Korteling, and K. P. Jackson, *Phys. Rev. C* **29**, 1806 (1984).
- [3] S. J. Yennello, K. Kwiatkowski, S. Rose, L. W. Woo, S. H. Zhou, and V. E. Viola, *Phys. Rev. C* **41**, 79 (1990).
- [4] L. G. Moretto, *Nucl. Phys.* **A247**, 211 (1975).
- [5] J. Gomez del Campo, *Phys. Rev. Lett.* **61**, 290 (1988).
- [6] W. G. Lynch and W. A. Friedman, *Phys. Rev. C* **28**, 16 (1983); **28**, 950 (1983).
- [7] M. Blann, T. Komoto, and I. Tserruya, *Phys. Rev. C* **40**, 2498 (1989).
- [8] D. H. Boal and R. M. Woloshyn, *Phys. Rev. C* **20**, 1878 (1979).
- [9] R. E. L. Green, K. P. Jackson, and R. G. Korteling, *Phys. Rev. C* **25**, 828 (1982).
- [10] H. Sakai, K. Hosono, N. Matsuoka, S. Nagamachi, K. Okada, K. Maeda, and H. Shimzu, *Nucl. Phys.* **A344**, 41 (1980).
- [11] Z. Lewandowski, E. Loeffler, R. Wagner, H. H. Mueller, W. Reichart, and P. Schober, *Nucl. Phys.* **A389**, 247 (1982).
- [12] T. Tamura, H. Lenske, and T. Ugadawa, *Phys. Rev. C* **23**, 2769 (1981).
- [13] A. M. Zebelman, A. M. Poskanzer, J. D. Bowman, R. G. Sextro, and V. E. Viola, *Phys. Rev. C* **11**, 1280 (1975).
- [14] W. Trautmann, K. D. Hildenbrand, U. Lynen, W. F. J. Müller, H. J. Rabe, H. Sann, H. Stelzer, R. Trockl, R. Wada, N. Brummund, R. Glasow, K. H. Kampert, R. Santo, E. M. Eckert, J. Pochodzalla, I. Bock, and D. Pelte, *Nucl. Phys.* **A471**, 191c (1987).
- [15] D. J. Fields, W. G. Lynch, C. B. Chitwood, C. K. Gelbke, M. B. Tsang, H. Utsonomiya, and J. Aichelin, *Phys. Rev. C* **30**, 1912 (1984).
- [16] N. R. Yoder, Indiana University Cyclotron Facility Internal Report No. 85-4, 1985; C. R. Gould and N. R. Robertson, *IEEE Trans. Nucl. Soc.* **NS-30**, 3758 (1985).
- [17] J. Lisantti, J. R. Tinsley, D. M. Drake, I. Berquist, L. W. Swenson, D. K. M. Daniels, F. E. Bertrand, E. E. Gross, D. J. Horan, and T. P. Sjoreen, *Phys. Lett.* **147B**, 23 (1984).
- [18] R. Bond, P. J. Johansen, S. E. Koonin, and S. Garpman, *Phys. Lett.* **71B**, 43 (1977).
- [19] T. C. Awes, G. Poggi, C. K. Gelbke, B. B. Back, B. G. Glagola, H. Breuer, and V. E. Viola, Jr., *Phys. Rev. C* **24**, 89 (1981).
- [20] D. E. Fields, K. Kwiatkowski, D. Bonser, R. W. Viola, V. E. Viola, W. G. Lynch, J. Pochodzalla, M. B. Tsang, C. K. Gelbke, D. J. Fields, and Sam. M. Austin, *Phys. Lett. B* **220**, 356 (1989).
- [21] J. L. Wile, D. E. Fields, K. Kwiatkowski, S. J. Yennello, K. B. Morley, E. Renshaw, S. Reed, V. E. Viola, N. Carlin, C. K. Gelbke, W. G. Gong, W. G. Lynch, M. B. Tsang, and H. M. Xu, Indiana University Nuclear Chemistry Report No. INC-40007-77, 1990.
- [22] W. A. Friedman and W. G. Lynch, *Phys. Rev. C* **28**, 950 (1983); **28**, 16 (1983).